BIOCHEMISTRY
including biophysical chemistry & molecular biology

Article

pubs.acs.org/biochemistry

Amilorides Bind to the Quinone Binding Pocket of Bovine Mitochondrial Complex I

Masatoshi Murai, Sonomi Murakami, Takeshi Ito, and Hideto Miyoshi*

Division of Applied Life Sciences, Graduate School of Agriculture, Kyoto University, Sakyo-ku, Kyoto 606-8502, Japan

Supporting Information

ABSTRACT: Amilorides, well-known inhibitors of Na^+/H^+ antiporters, were previously shown to inhibit bacterial and mitochondrial NADH-quinone oxidoreductase (complex I) but were markedly less active for complex I. Because membrane subunits ND2, ND4, and ND5 of bovine complex I are homologous to Na^+/H^+ antiporters, amilorides have been thought to bind to any or all of the antiporter-like subunits; however, there is currently no direct experimental evidence that supports this notion. To identify the binding site of amilorides in bovine complex I, we synthesized two photoreactive amilorides (PRA1 and PRA2), which have a photoreactive azido ($-N_3$) group and terminal alkyne ($-C{\equiv}CH$) group at the opposite ends of the molecules, respectively, and conducted photoaffinity labeling with bovine heart submitochondrial particles. The terminal alkyne group allows various molecular tags to covalently attach to it via Cu^+-catalyzed click chemistry, thereby allowing purification and/or detection of the labeled peptides. Proteomic analyses revealed that PRA1 and PRA2 label none of the antiporter-like subunits; they specifically label the accessory subunit B14.5a and core subunit 49 kDa (N-terminal region of Thr25−Glu115), respectively. Suppressive effects of ordinary inhibitors (bullatacin, fenpyroximate, and quinazoline), which bind to the putative quinone binding pocket, on labeling were fairly different between the B14.5a and 49 kDa subunits probably because the binding positions of the three inhibitors differ within the pocket. The results of this study clearly demonstrate that amilorides inhibit complex I activity by occupying the quinone binding pocket rather than directly blocking translocation of protons through the antiporter-like subunits (ND2, ND4, and ND5). The accessory subunit B14.5a may be located adjacent to the N-terminal region of the 49 kDa subunits. The structural features of the quinone binding pocket in bovine complex I were discussed on the basis of these results.

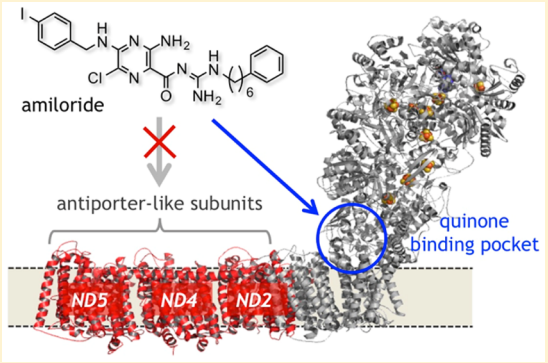

The proton-pumping NADH-quinone oxidoreductase (complex I) couples the transfer of electrons from NADH to quinone with the translocation of protons across the membrane, which drives energy-consuming processes such as ATP synthesis.[1,2] Complex I is the largest of the respiratory-chain enzymes; for example, the enzyme from bovine heart mitochondria is composed of 14 central subunits and a large number of accessory subunits with a total molecular mass of ∼1 MDa.[3] The crystal structures of entire complex I from *Thermus thermophilus*[4] and *Yarrowia lipolytica*[5] were determined at 3.3 and 3.6 Å, respectively, providing useful structural information about the mechanism underlying coupling between electron transfer and proton translocation in the enzyme. Together with the crystal structure of the membrane domain of *Escherichia coli* complex I,[6] possible pathways of proton translocation in subunits Nqo12 (NuoL in *E. coli*, ND5 in bovine), Nqo13 (NuoM, ND4), and Nqo14 (NuoN, ND2) have been proposed.[4] Because the Nqo12−Nqo14 subunits are homologous to members of the Mrp Na^+/H^+ antiporter family,[7] their mechanisms of ion translocation may be related. With regard to this point, it is noteworthy that the "deactive" form of bovine heart complex I has been reported to exhibit Na^+/H^+ antiporter activity.[8]

Detailed studies of the action mechanism of specific inhibitors of complex I have provided structural and functional insights into the ubiquinone reduction and the proton translocation in this enzyme.[1,2,9] Photoaffinity labeling studies using complex I inhibitors produced valuable insights into the binding sites of the inhibitors/quinone.[10−15] Earlier photoaffinity labeling studies indicated that the binding sites of inhibitors reside at the interface between the hydrophilic domain and membrane domain, including the 49 kDa, PSST, and ND1 subunits. The peptides identified by photoaffinity labeling studies[11−15] are included in a long narrow quinone access cavity suggested by the crystal structure of *T. thermophilus* complex I.[4] On the other hand, extensive mutagenesis studies using yeast *Y. lipolytica* complex I indicated that the reduction of ubiquinone by electrons from Fe−S cluster N2 may occur in the large pocket composed of the 49 kDa and PSST subunits; however, the specific binding sites for ubiquinone and different inhibitors may not be identical.[16,17]

Received: February 24, 2015
Revised: April 6, 2015
Published: April 7, 2015

DOI: 10.1021/acs.biochem.5b00187
Biochemistry 2015, 54, 2739−2746

Although electron densities corresponding to bound decyl-ubiquinone and piericidin A were detected at the deep end of the long narrow cavity of *T. thermophilus* complex I,[4] the independent structure of the bound enzyme has not been described.[2] Zickermann et al. modeled the location of the planar aromatic ring of quinazoline-type inhibitors to the position between the tip of the $\beta_1-\beta_2$ loop of the 49 kDa subunit and Met91 of the PSST subunit in *Y. lipolytica* complex I,[5] which is fairly farther from cluster N2 compared to the location of the quinone headgroup proposed for *T. thermophilus* complex I.[4]

Amilorides are well-known inhibitors of Na^+/H^+ and Na^+/Ca^{2+} antiporters and Na^+ channels.[18,19] The structural characteristics of amilorides that are critical for their inhibitory activities vary greatly depending on different ion transporters and species.[18] Amilorides were previously shown to inhibit bacterial and mitochondrial complex I,[20,21] whereas their inhibitory potencies, in terms of IC_{50} values, were markedly weaker than those of traditional inhibitors such as rotenone, piericidin A, and acetogenins. Because the membrane subunits ND2, ND4, and ND5 (in bovine complex I) are homologous to the subunits from the Mrp family of Na^+/H^+ antiporters,[7] amilorides have been thought to block complex I activity by binding to any or all of the antiporter-like subunits; however, there is currently no direct experimental evidence to support this notion. If this is the case, the modes of action of amilorides need to be examined in more detail because they may become useful molecular tools in the study of the mechanism underlying translocation of protons through the antiporter-like subunits.

To identify the binding site of amilorides in bovine complex I, we conducted photoaffinity labeling experiments using two recently produced photoreactive amilorides (PRA1 and PRA2, Figure 1, ref 22) with bovine heart submitochondrial particles (SMP). Proteomic analyses revealed that PRA1 and PRA2 specifically label to the hydrophilic accessory subunit B14.5a and core subunit 49 kDa (N-terminal region of Thr25–Glu115), respectively. Our results revealed that amilorides inhibit complex I activity by disturbing the function of the interface between the hydrophilic domain and membrane domain rather than directly blocking translocation of protons through the antiporter-like subunits (ND2, ND4, and ND5).

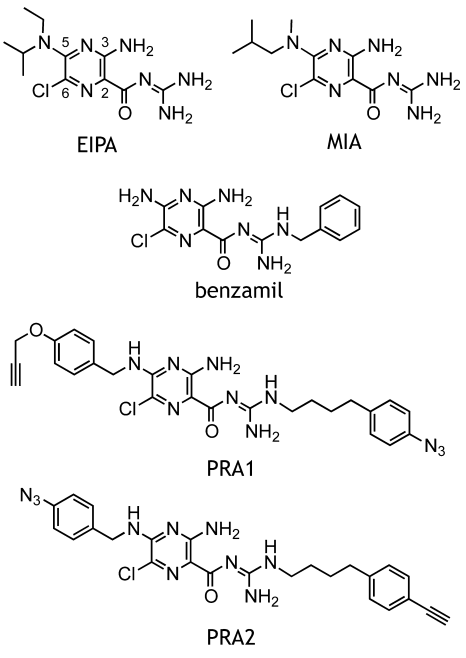

Figure 1. Structures of the compounds used in this study.

EXPERIMENTAL PROCEDURES

Materials. *T. thermophilus* membrane preparations were kindly provided by K. Yokoyama (Kyoto Sangyo University, Kyoto, Japan). Fenpyroximate was a kind gift from Nihon Nohyaku Co. Ltd. (Tokyo, Japan). Aminoquinazoline was the same as that used in the previous study.[23] The photoreactive amilorides PRA1 and PRA2 were synthesized as reported previously.[22] The cleavable biotin-SS-azido (Figure S1 of the Supporting Information) was synthesized as described previously.[24] Protein standards (Precision Plus Protein Standards and Precision Plus Protein Dual Xtra Standards) for SDS–PAGE were purchased from Bio-Rad (Hercules, CA). The Click-iT reaction buffer kit and TAMRA-azido (Figure S1 of the Supporting Information) were purchased from Life Technologies (Carlsbad, CA). The goat anti-human NDUFA7 (bovine B14.5a counterpart) antibody (catalog no. SAB2052106) was purchased from Sigma-Aldrich (St. Louis, MO). The chicken anti-bovine ND3 antibody was raised by Sigma-Aldrich Japan Genosys (Tokyo, Japan) against the synthetic peptide SLAYEWTQKGLEWTE, which corresponds to the C-terminal region of the bovine ND3 subunit. Other reagents were all of analytical grade.

Preparation of Bovine Heart SMP and General Procedures for Photoaffinity Labeling. Bovine heart SMP were prepared from isolated bovine heart mitochondria by the method of Matsuno-Yagi and Hatefi[25] and stored in a buffer containing 250 mM sucrose and 10 mM Tris-HCl (pH 7.4) at −80 °C until being used. NADH oxidase and NADH-Q_1 oxidoreductase activities in SMP were measured according to the procedures described previously.[26]

In the photoaffinity labeling study, bovine SMP (1.0 mg of proteins/mL, 100–250 μL) were incubated with the indicated concentration of PRA1 or PRA2 in a buffer containing 250 mM sucrose, 1 mM $MgCl_2$, and 50 mM KP_i (pH 7.4) for 10 min and then photoirradiated with a long wavelength UV lamp (Black-Ray model B-100A, UVP, Upland, CA) for 10 min on ice. SMP were collected by ultracentrifugation (20000*g* for 20 min at 4 °C) and subjected to further analyses.

Electrophoresis. PRA1- or PRA2-labeled SMP were solubilized in a sample buffer containing 50 mM Bistris-HCl (pH 7.2), 50 mM NaCl, 10% (w/v) glycerol, 1% (w/v) DDM, and 0.001% (w/v) Ponceau S for 1 h on ice, and the supernatant was separated by Blue Native (BN)-PAGE using a 4 to 16% precast gel system (Life Technologies, Carlsbad, CA) according to the manufacturer's protocol. Complex I was isolated by electroelution using a model 422 Electro-Eluter (Bio-Rad), denatured in 50 mM Tris-HCl buffer (pH 8.0) containing 1% (w/v) SDS, and conjugated with a TAMRA-azido tag via Cu^+-catalyzed click chemistry.[24] The TAMRA-attached complex I was resolved on a Laemmli-type 12.5% SDS gel[27] or Schägger-type 10% SDS gel containing 6.0 M urea.[28]

During doubled SDS–PAGE (dSDS–PAGE), the proteins were resolved via two-dimensional electrophoresis using 10 and 16% Schägger-type SDS gels according to the procedures described previously.[15,29] The migration pattern of fluorescent protein was visualized by the model FLA-5100 (Fuji Film, Tokyo, Japan) or Typhoon FLA9500 (GE Healthcare,

DOI: 10.1021/acs.biochem.5b00187
Biochemistry 2015, 54, 2739–2746

Buckinghamshire, U.K.) Bioimaging analyzer using a 532 nm light source and an LPG (575 nm) filter. Data processing and quantification of fluorescence were conducted using Multi Gauge (Fuji Film) and Image Quant (GE Healthcare) software, respectively.

Immunochemical Analysis. To enrich the labeled proteins, SMP (1.0 mg of proteins/mL, total of 0.4−1.0 mg) were labeled with 10 μM PRA1, denatured in a 50 mM Tris-HCl buffer (pH 8.0) containing 1% (w/v) SDS, and conjugated with the cleavable biotin-SS-azido via Cu^+-catalyzed click chemistry. The biotinylated proteins were captured on streptavidin-agarose in Tris-buffered saline (TBS buffer) containing 1% (w/v) Triton X-100 at a protein concentration of ∼0.9 mg/mL and released in a Schägger-type SDS−PAGE sample buffer containing 2.5% mercaptoethanol.[24]

To detect the specific complex I subunits, proteins were separated on a Schägger-type SDS gel and transferred onto a PVDF membrane according to the conditions described elsewhere.[13,15] The membrane was blocked with 1% (w/v) gelatin in TBS buffer containing 0.5% (w/v) Tween 20 (Tween TBS) and then probed with appropriate primary antibody, followed by an incubation with the corresponding alkaline-phosphatase-conjugated secondary antibody. The membrane was washed three times with Tween TBS and developed with NBT/BCIP colorimetric reagents (Bio-Rad). Primary and secondary antibodies to complex I subunits were diluted with Tween TBS at the following ratios: chicken anti-bovine ND3, 1:4000; goat anti-human NDUFA7 (bovine B14.5a), 1:4000; and goat anti-chicken and rabbit anti-goat secondary antibodies conjugated with alkaline phosphatase (Sigma-Aldrich), 1:8000.

Limited Proteolysis of the 49 kDa Subunit. Partial digestion of the PRA2-labeled 49 kDa subunit was conducted according to the procedures previously described[15,30] using V8 protease and a 15% Tris-EDTA SDS−PAGE mapping gel. The V8 digestion was allowed to continue for 30 min at room temperature. The digests were subjected to fluorescent gel imaging and CBB staining.

For exhaustive digestion of the labeled 49 kDa subunit, the subunit was isolated by electroelution and exhaustively digested using lysylendopeptidase (Lys-C, Wako Pure Chemicals, Osaka, Japan), endoprotease Asp-N (Loche, Penzburg, Germany), or trypsin (Promega) in 50 mM Tris-HCl buffer (containing 0.1% SDS), 50 mM sodium phosphate buffer (containing 0.01% SDS), or ammonium bicarbonate buffer (containing 0.01% SDS).[15] The digests were analyzed by Tricine/SDS−PAGE (16.5% T, 6% C).

Mass Spectrometric Analysis. To identify complex I subunits, the proteins were digested "in gel" by trypsin and identified by a nano-LC (ADVANCE UHPLC SYSTEM, Michrom BioResources) and MS (LTQ Orbitrap XL, Thermo Fisher Scienticic) system equipped with L-column micro (0.1 mm × 150 mm, Chemicals Evaluation and Research Institute) at the APRO Life Science Institute, Inc. (Tokushima, Japan). The digests were separated by reverse-phase chromatography at a flow rate of 500 nL/min. The mobile phase consisted of the changing gradient of 0.1% (w/v) aqueous formic acid and acetonitrile. The data collected were compared against NCBInr using Mascot (Matrix Science) and analyzed by Scafford (Proteome Software).

Protein digests were also characterized by a Bruker Autoflex III Smartbeam instrument (MALDI-TOF/TOF) according to the same procedures as described previously.[15]

RESULTS

Synthesis of Photoreactive Amilorides (PRA1 and PRA2). The inhibitory activities of commercially available amilorides (EIPA, MIA, and benzamil) were determined with the NADH oxidase assay in SMP, and their IC_{50} values were approximately 20−30 μM, being comparable to those reported previously.[20] As part of the photoaffinity labeling technique, less nonspecific binding occurred with the higher binding affinities of photoreactive ligands; therefore, the use of a ligand with a binding affinity as high as possible allows the accurate interpretation of data obtained in the photoaffinity labeling experiments. From this point of view, commercially available amilorides were not suitable as templates for designing photoreactive amilorides; hence, we needed to produce much more potent amiloride derivatives.

We recently synthesized numerous amilorides, conducted a structure−activity relationship study, and successfully produced two photoreactive amilorides [PRA1 and PRA2 (Figure 1)].[22] An azido group and terminal alkyne (-C≡CH) were incorporated into both inhibitors as a photoreactive group and "footing" for sequential Cu^+-catalyzed click chemistry, respectively, but at opposite ends in the molecules. We confirmed that PRA1 (IC_{50} = 0.25 ± 0.04 μM) and PRA2 (IC_{50} = 0.30 ± 0.07 μM) both maintain the potent inhibitory activities, which are approximately 100-fold more potent than those of commercially available amilorides.

Photoaffinity Labeling of Bovine Complex I with PRA1 or PRA2. Bovine SMP (1.0 mg of proteins/mL) were incubated with 10 μM PRA1 or PRA2 and irradiated with a UV lamp, and the labeled complex I was isolated by preparative BN-PAGE and electroelution. To visualize the labeled subunits, the isolated complex I was covalently conjugated with a fluorescent TAMRA tag (Figure S1 of the Supporting Information) via Cu^+-catalyzed click chemistry, followed by its resolution on an SDS gel. As shown in Figure 2A, complex I labeled by PRA1 afforded a major fluorescent band with an apparent molecular mass of ∼15 kDa on a 10% Schägger-type SDS gel. On the other hand, complex I labeled by PRA2 gave a fluorescent band at ∼50 kDa on a 12.5% Laemmli-type SDS gel (Figure 2B). Judging from fluorescence intensities of these two bands, the labeling yield of PRA2 was significantly lower than that of PRA1. This does not necessarily indicate that the binding affinity of PRA2 for the enzyme is lower than that of PRA1 because the labeling yield is also affected by the reactivity of the local protein microenvironment interacting with the photoreactive azido group. The presence of NADH (100 μM) during UV irradiation did not affect the extent of labeling by either of the amilorides (data not shown). In addition, a good correlation was found between the labeling of the ∼15 kDa protein and the inhibition of the NADH oxidase activity for PRA1 (Figure S2 of the Supporting Information).

Some potent amilorides synthesized in our laboratory (e.g., **5n** in ref 22) also inhibited complex I in *T. thermophilus* membrane preparations, which has no accessory subunit. This finding means that amilorides bind to the core subunit(s) of bovine complex I; hence, at least one of the two labeled proteins (the ∼15 and ∼50 kDa proteins) is the core subunit. Moreover, because the chemical structures of PRA1 and PRA2 are similar, except for the position of a photolabile azido group, it is likely that these two subunits are adjacent to each other.

The PRA2-labeled ∼50 kDa band was easily identified as the hydrophilic 49 kDa subunit by MALDI-TOF MS of its tryptic

DOI: 10.1021/acs.biochem.5b00187
Biochemistry 2015, 54, 2739−2746

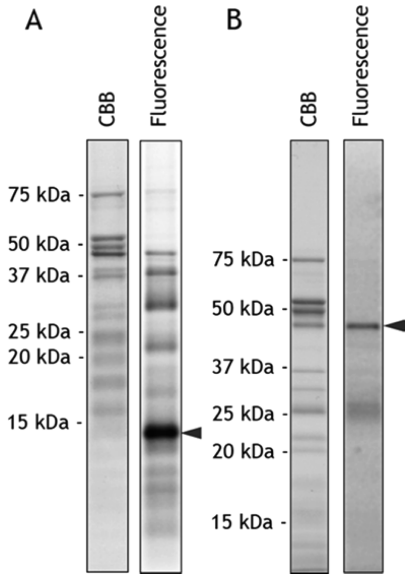

Figure 2. Photoaffinity labeling of bovine complex I by PRA1 or PRA2. Bovine SMP (1.0 mg of proteins/mL) were labeled with PRA1 or PRA2 (10 μM each), followed by isolation using preparative BN-PAGE and electroelution. The isolated complex I was conjugated with the fluorescent TAMRA tag via Cu^{+}-catalyzed click chemistry. The PRA1- or PRA2-labeled complex I (equivalent to 250 μg of SMP proteins) was separated on a 10% Schägger-type SDS gel (A) or a 12.5% Laemmli-type SDS gel (B), respectively. They were then subjected to fluorescent gel imaging and CBB staining.

digests (41% coverage) because the subunit was clearly resolved as a single band on a 12.5% SDS gel. However, among the bovine complex I subunits, those that migrated in the ~15 kDa region contained multiple proteins, including the hydrophobic ND3 subunit and several metazoan-specific accessory subunits. Regardless, it is noteworthy that the photoreactive amilorides labeled none of the antiporter-like subunits (ND2, ND4, and ND5), which have been believed to be the targets of amilorides.

Characterization of the ~15 kDa Protein Labeled by PRA1. To characterize the ~15 kDa protein, the PRA1-labeled complex I was further resolved by dSDS−PAGE, two-dimensional electrophoresis using 10 and 16% Schägger-type SDS gels.[29] dSDS−PAGE is useful for separating highly hydrophobic ND subunits from other hydrophilic subunits, including the accessory subunits. The PRA1-derived fluorescent spot migrated on a diagonal axis on the two-dimensional gel (Figure 3A, right), while Western analysis using the anti-bovine ND3 antibody revealed that the ND3 subunit migrates separately from the diagonal axis (Figure 3B, left), like other hydrophobic subunits such as the ND5 and ND4 subunits. The PRA1-labeled protein, which was attached by an azido-containing biotin tag,[24] was enriched using immobilized streptavidin agarose. This protein did not immunologically react with the anti-bovine ND3 antibody (data not shown). These results were sufficient to exclude the ND3 subunit as a candidate for the PRA1-labeled subunit.

The silver-stained spot corresponding to the fluorescent spot on the dSDS−PAGE gel (Figure 3A, left) was excised from the

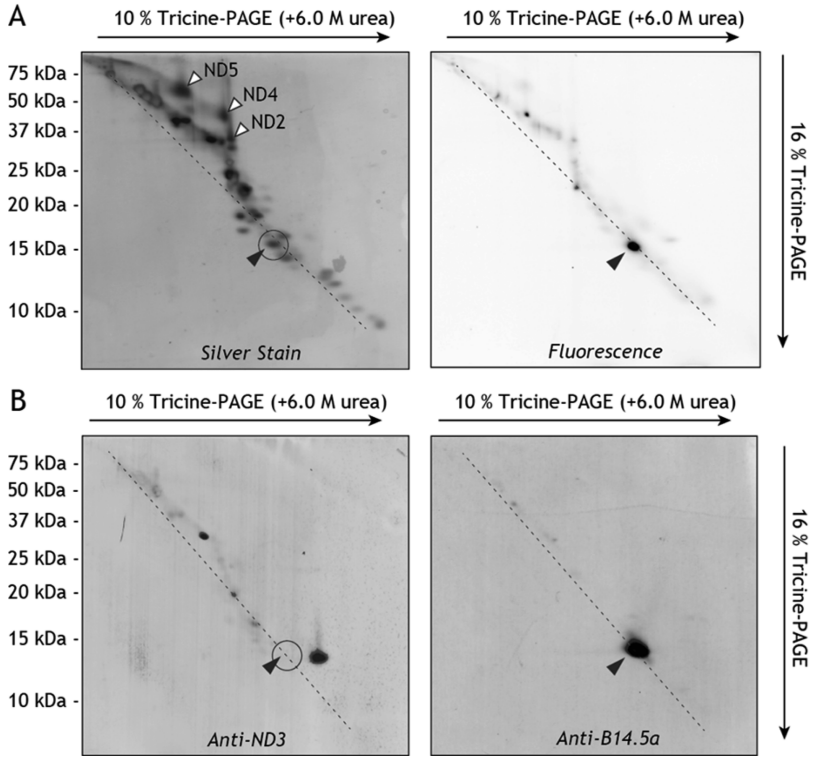

Figure 3. Resolution of the PRA1-labeled complex I by dSDS−PAGE. The PRA1-labeled complex I (equivalent to 400 μg of SMP proteins) was prepared and conjugated with a fluorescent TAMRA tag using the same procedures that are described in the legend of Figure 2. The fluorescently tagged complex I was separated on a one-dimensional 10% Schägger-type tricine gel (10% T and 3% C, containing 6.0 M urea), followed by two-dimensional separation on a 16% Schägger-type gel (16% T, 3% C). (A) Proteins were visualized by a silver stain (left) or subjected to fluorescent gel imaging (right). (B) The proteins separated by dSDS−PAGE were, alternatively, transferred onto a PVDF membrane, confirmed with an anti-bovine ND3 (left) or anti-human B14.5a (right) antibody, followed by colorimetric detection using appropriate alkaline-phosphate-conjugated secondary antibodies.

DOI: 10.1021/acs.biochem.5b00187
Biochemistry 2015, 54, 2739−2746

gel and digested "in gel" with trypsin, and the digests were analyzed by LC−MS. The tryptic digests contained the peptides derived from five complex I subunits, including B14.5a, B14.5b, B13, B14.7, and 15 kDa (Table S1 of the Supporting Information).

According to the model of the subunit assembly of *Y. lipolytica* complex I,[31] the B14.5b, B14.7, and 15 kDa subunits are included in the distal proton-pumping module (P_D module) in the membrane domain. Because PRA2 specifically bound to the 49 kDa subunit, as described above, it is reasonable to assume that PRA1 bound to the subunit adjacent to the 49 kDa subunit. Therefore, the ∼15 kDa protein is none of the three subunits in the P_D module. The structure of bovine complex I was recently determined at a resolution of 5 Å by single-particle electron cryo-microscopy.[32] On the basis of this structural model, the B13 subunit was assigned to the side of the 30 kDa subunit, which is located at the opposite side of the putative entry point from the quinone binding cavity. Accordingly, B14.5a is a possible candidate for the PRA1-labeled protein, although its location is still unknown.

To verify this, SMP were labeled by 10 μM PRA1, followed by the attachment of a cleavable biotin-SS-azido (Figure S1 of the Supporting Information) via Cu^+-catalyzed click chemistry. The biotinylated protein was captured on immobilized streptavidin-agarose and released under mild reaction conditions using Shägger's SDS−PAGE sample buffer containing 2.5% mercaptoethanol. These procedures were monitored by the anti-human NDUFA7 antibody, which cross-reacts with the bovine counterpart B14.5a subunit (Figure 4). Western analysis clearly indicated that the ∼15 kDa protein labeled by PRA1 is the accessory subunit B14.5a. Using the same antibody, we also confirmed that the fluorescent spot migrated on the diagonal axis on a two-dimensional gel is the B14.5a subunit (Figure 3B, right).

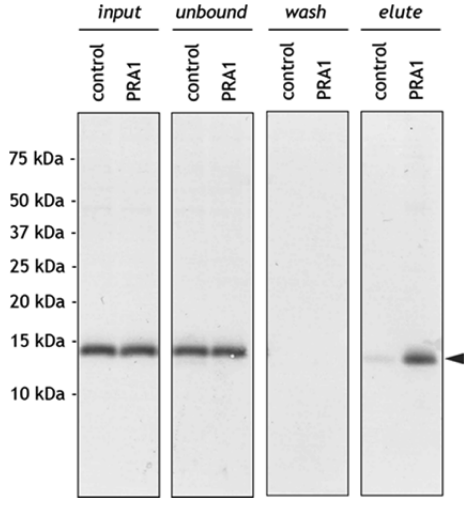

Figure 4. Enrichment and identification of the PRA1-labeled protein. Bovine SMP (2.0 mg of proteins/mL, total 1 mg of proteins) were labeled by PRA1 (10 μM) and conjugated with cleavable biotin-SS-azido[24] via Cu^+-catalyzed click chemistry. The biotinylated protein was enriched using streptavidin-agarose and released in Schägger's SDS−PAGE sample buffer, according to the procedure described in Experimental Procedures. Specific capture/release procedures were monitored by Western analysis using an anti-B14.5a antibody on a 10% Schägger-type tricine gel (10% T and 3% C, containing 6.0 M urea).

Localization of the Labeled Sites in 49 kDa and B14.5a Subunits. To roughly localize the PRA2-labeled site, the PRA2-labeled 49 kDa subunit was isolated from a Laemmli-type 12.5% SDS gel, attached by the TAMRA tag, and then partially digested in gel with V8 protease according to the previously described procedure.[14,15] Partial V8 digestion reproductively provided two fluorescent bands on a 15% Tris-EDTA mapping gel, which converged on ∼20 and ∼10 kDa fragments (Figure 5A). The former and latter fragments

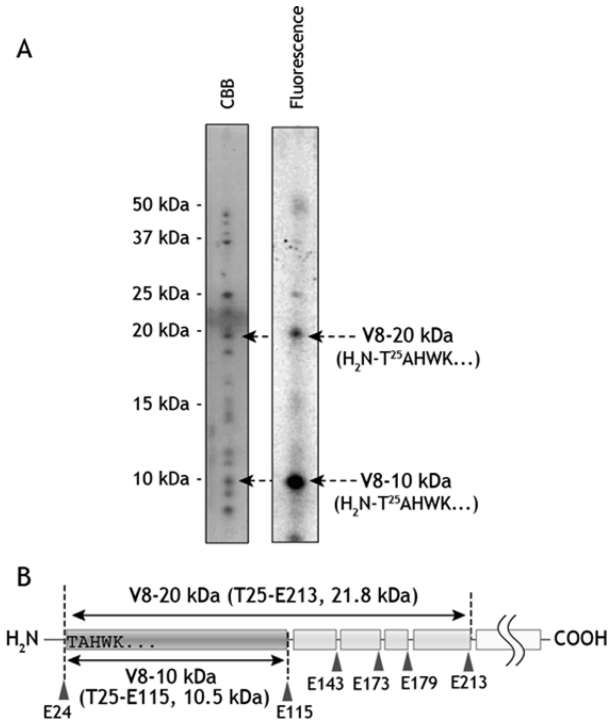

Figure 5. Proteomic analysis of the PRA2-labeled site in the 49 kDa subunit. Complex I, which was labeled by 10 μM PRA2, was isolated by preparative BN-PAGE and conjugated with the fluorescent TAMRA tag via Cu^+-catalyzed click chemistry, followed by SDS−PAGE on a 12.5% Laemmli-type SDS gel. (A) The CBB-stained gel piece of the 49 kDa subunit was digested in gel with V8 protease (i.e., Cleveland mapping). The N-terminal sequences, determined by Edman degradation, of the CBB-stained bands corresponding to the fluorescent bands are shown. (B) Schematic presentation of protease digestion of the 49 kDa subunit. The predicted cleavage sites are denoted with arrows and indicated by their residue numbers in the mature sequences of the bovine 49 kDa subunit (SwissProt entry P17694).

were assigned to the regions of Thr25−E213 (21.8 kDa) and Thr25−Glu115 (10.5 kDa), respectively (Figure 5B), because (i) the N-terminal sequences of the V8 digests of the 49 kDa subunit have been extensively determined in our previous studies[14,15] and (ii) the digests were found to contain the internal sequence T^{95}YLQALPYFDR^{105} in common [identified by MALDI-TOF/TOF (Figure S3 of the Supporting Information)].

To pinpoint the position labeled by PRA2, we conducted peptide mapping for the peptide fragments, which were formed by exhaustive digestion by V8 protease, Lys-C, or trypsin. However, we were unable to detect any fluorescent spot on the SDS gel. This was attributed to the low labeling yield of PRA2 and, hence, an identification limitation of fluorescence. We

DOI: 10.1021/acs.biochem.5b00187
Biochemistry 2015, 54, 2739−2746

conducted exhaustive digestion under various reaction conditions; however, peptide mapping did not improve.

The peptide mapping of the labeled B14.5a subunit exhaustively digested by Lys-C, Asp-N, or trypsin was also unsuccessful because the digests provided were too small (~3 kDa) on the tricine gel to theoretically predict the labeled region.

Effects of Ordinary Complex I Inhibitors on Labeling by PRA1 or PRA2. To determine whether the labeling of the B14.5a and 49 kDa subunits by PRA1 and PRA2, respectively, is affected by ordinary complex I inhibitors, bovine SMP were UV-irradiated with 10 μM PRA1 or PRA2 in the presence of 10 μM bullatacin, fenpyroximate, or aminoquinazoline, each of which binds to the putative quinone binding pocket,[10−15] followed by the attachment of a fluorescent TAMRA-azido tag via Cu^+-catalyzed click chemistry for visualization. The concentration (10 μM) of these competitors was set to be largely in excess of that giving the complete inhibition of the enzyme activity. Additionally, considering differences in binding affinities (in terms of the IC_{50} values) between the amilorides and the competitors, this concentration is sufficiently high to block the labeling if they compete with each other.

The specific labeling of the 49 kDa subunit by PRA2 was completely suppressed in the presence of bullatacin, fenpyroximate, and aminoquinazoline (Figure 6A). On the other hand,

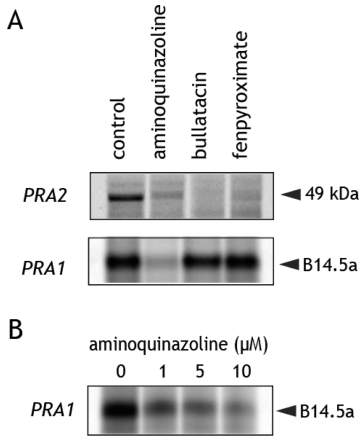

Figure 6. Effects of ordinary complex I inhibitors on the specific labeling of complex I by PRA1 or PRA2. (A) SMP (1.0 mg of proteins/mL) were incubated with 10 μM PRA1 or PRA2 in the presence of 10 μM bullatacin, fenpyroximate, or aminoquinazoline. The PRA1- or PRA2-labeled complex I was isolated by BN-PAGE, conjugated with the fluorescent TAMRA tag via Cu^+-catalyzed click chemistry, and separated on a Schägger- or Laemmli-type SDS gel, respectively. (B) Effects of aminoquinazoline on the labeling of the B14.5a subunit by PRA1. SMP (1.0 mg of proteins/mL) were incubated with 10 μM PRA1 in the presence of the indicated concentrations of aminoquinazoline. Data are representative of three independent experiments.

the labeling of the B14.5a subunit by PRA1 was suppressed by aminoquinazoline, but not by bullatacin or fenpyroximate (Figure 6A). We confirmed that this suppression by aminoquinazoline is concentration-dependent (Figure 6B). We did not use higher concentrations of bullatacin or fenpyroximate because high concentrations of hydrophobic chemicals nonspecifically disturb the enzyme and/or membrane environment. This difference must reflect differences in the binding positions of the three inhibitors within the quinone binding pocket, as discussed later. We note that the labeling of the B14.5a and 49 kDa subunits was completely suppressed in the presence of an amiloride analogue [25 μM **5n** (Figure S4 of the Supporting Information)], the IC_{50} value of which is almost identical to those of PRA1 and PRA2. A short-chain quinone analogue Q_2 suppressed the labeling of the B14.5a and 49 kDa subunits by ~60 and ~20%, respectively, at 50 μM (Figure S4 of the Supporting Information). This is probably because the binding affinities are largely different between PRA1/PRA2 and Q_2.

■ DISCUSSION

Ever since amilorides were reported to inhibit bacterial and mitochondrial complex I,[20,21] they have been considered to bind to any or all of the Na^+/H^+ antiporter-like subunits of the enzyme solely because amilorides are potent inhibitors of Na^+/H^+ antiporters.[18,19] However, this study clearly reveals that amilorides bind to none of the antiporter-like subunits; they occupy the quinone binding pocket of the enzyme. The pyrazine ring and alkyl side-chain moiety bound to the core subunit 49 kDa and the hydrophilic accessory subunit B14.5a, respectively. Unfortunately, pinpoint identification of the labeled positions in both subunits was unsuccessful. Nevertheless, as the C-terminal half of the identified region in the 49 kDa subunit (Thr25−Glu115) is densely surrounded by the TYKY, 30 kDa, and another part of the 49 kDa subunit itself,[4,5] it may not contain the binding site of PRA2. Binding of the pyrazinoyl guanidine moiety to the 49 kDa subunit must be the main cause for disturbing the enzyme function because (i) this skeleton is a critical toxophore of amilorides[22] and (ii) the N-terminal half of the region (Thr25−Glu115) labeled by PRA2 overlaps that labeled by a quinazoline-type inhibitor, which binds to the interface between the N-terminal region (Asp41−Arg63) of the 49 kDa subunit and the third matrix side loop of the ND1 subunit.[11,14]

In this study, we first observed the labeling of an accessory subunit among numerous photoaffinity labeling studies with bovine complex I using various types of inhibitors.[10−15,33,34] The structures, locations around the core subunits, and functions (if any) of the accessory subunits of mitochondrial complex I remain largely unknown. Although a recent structural model of bovine complex I determined by single-particle electron cryo-microscopy assigned the location of some accessory subunits,[32] the B14.5a subunit, which is predicted to have no transmembrane helix, was not assigned in the study. PRA1 and PRA2, which are very similar in structure, but have a photoreactive azido group at the opposite ends of the molecules, labeled the 49 kDa and B14.5a subunits, respectively. The most straightforward explanation for this result may be that the location of B14.5a is adjacent to the N-terminal region of the 49 kDa subunit. This position is far from the putative entry point into the quinone binding cavity.[4]

Baradaran et al. proposed that the quinone binding pocket of *T. thermophilus* complex I (an ~30 Å long cavity), which is composed of Nqo4 (49 kDa), Nqo6 (PSST), and Nqo8 (ND1), is completely enclosed from the outer medium with a narrow entry point in the membrane.[4] The recently reported crystal structure of mitochondrial complex I from *Y. lipolytica* showed that the structural characteristics of the quinone binding pocket of this enzyme, including the location of its entry point, are basically similar to those of *T. thermophilus* complex I; however, some distinct features were observed in the $\beta_1-\beta_2$ loop of the 49 kDa subunit, the loop connecting TMH5 and TMH6 of ND1, and the loop connecting TMH1

DOI: 10.1021/acs.biochem.5b00187
Biochemistry 2015, 54, 2739−2746

and TMH2 of ND3.[5] According to the sequence alignment for the bovine 49 kDa subunit and *T. thermophilus* Nqo4 subunit, the N-terminal half of the region of Thr25−Glu115 (Glu8−Asp94 in *T. thermophilus* complex I) is located on the top of the third matrix loop of the ND1 subunit, which connects TMH5 and TMH6 and forms an inner part of the putative quinone binding pocket (Figure S4 of the Supporting Information). We found that PRA1 specifically labels the accessory subunit B14.5a. Because the 14 central subunits that harbor the core function of energy conversion are conserved from bacteria to humans, the likelihood that the B14.5a subunit forms an inner part of the quinone binding cavity is low. Therefore, our result suggests that all of the PRA1 molecule is not necessarily accommodated within the pocket; namely, the alkyl side-chain moiety (at least the terminal end of it) may protrude from the quinone binding pocket and make contact with the B14.5a subunit. However, this idea is inconsistent with the proposal by Baradaran et al.[4] Considering the location of the N-terminal half of the region labeled by PRA2 (Figure S5 of the Supporting Information), our results may be explained by assuming that there is a fissure around the N-terminal region of the 49 kDa subunit, which faces the outer medium and is just too large to accommodate a small chemical (amiloride). We recently showed that a bulky ring-strained cycloalkyne possessing a rhodamine fluorophore (approximately 13 Å × 20 Å) directly reacts to the azido group incorporated into Asp160 in the 49 kDa subunit of intact complex I, which may be located in the inner part of the quinone binding cavity.[35] This finding suggests that there may be another access path into the cavity besides the putative narrow entry point. Thus, this study along with the previous work[35] does not support the proposed model in which the long and narrow quinone binding cavity is completely enclosed from the outer medium.

The labeling of 49 kDa subunits by PRA2 was completely suppressed by quinazoline, fenpyroximate, and bullatacin, which bind to the putative quinone binding pocket.[10−15] This result indicates that the toxophoric pyrazine ring of amilorides occupies a part of the quinone binding pocket. In contrast, the labeling of the B14.5a subunit by PRA1 was suppressed by quinazoline, but not by fenpyroximate or bullatacin even at concentrations that are largely in excess of that required for the complete inhibition of the enzyme activity. This difference must reflect differences in the binding positions of the three inhibitors within the quinone binding pocket, as demonstrated in the previous photoaffinity labeling studies.[10−15] Additionally, taking into consideration the fact that the position of the photoreactive azido group in PRA1 and PRA2 is on opposite ends of the long and flexible molecules, we cannot exclude the possibility that the suppressive effects arising from the competitors differ between the cross-linking reaction occurring at the toxophoric moiety and that occurring at the terminal end of the alkyl side chain.

A high concentration (100 μM) of amiloride analogue EIPA was reported to inhibit the transport of Na^+ by the *E. coli* NuoL subunit (ND5 in bovine) reconstituted into liposomes, which are composed of an *E. coli* membrane lipid mixture.[36] However, it is important to note that amilorides contain a guanidine moiety in their skeleton, which exhibits strong basicity; hence, a guanidine-HCl salt is often used as a denaturing reagent of proteins. The apparent inhibition reported by Steuber may have been due to nonspecific alterations in the nature of the NuoL subunit and/or membrane biophysical properties because of the high concentration of EIPA. In addition, amilorides are in an equilibrium state between protonated and nonprotonated forms at physiological pHs because their pK_a values generally range from 8 to 9.[18] Roberts and Hirst observed the significant uncoupling effect of EIPA due to its protonophoric ability in mitochondrial membrane,[8] as reported previously.[37] Thus, sufficient attention needs to be paid for the interpretation of experimental data obtained using high concentrations of amilorides.

In conclusion, we herein conducted the photoaffinity labeling using two photoreactive amilorides, PRA1 and PRA2, to identify the binding site of amilorides in bovine complex I. The results of this study revealed that PRA1 and PRA2 label none of the antiporter-like subunits; they specifically label the accessory subunit B14.5a and core subunit 49 kDa (N-terminal region Thr25−Glu115), respectively. Therefore, we concluded that amilorides inhibit the complex I activity by occupying the quinone binding pocket rather than blocking translocation of protons through the antiporter-like subunits (ND2, ND4, and ND5). The accessory subunit B14.5a may be located adjacent to the N-terminal region of the 49 kDa subunit.

■ ASSOCIATED CONTENT

Supporting Information

Structures of TAMRA-azido and biotin-SS-azido (Figure S1), correlation between the labeling and inhibition of enzyme activity (Figure S2), MALDI-TOF/TOF spectrum of a tryptic digest of the 49 kDa subunit (Figure S3), suppression of the labeling of the B14.5a and 49 kDa subunits by a synthetic amiloride (Figure S4), the location of the N-terminal half of the PRA2-labeled region (Figure S5), and proteins identified by LC−MS/MS analysis (Table S1). This material is available free of charge via the Internet at http://pubs.acs.org.

■ AUTHOR INFORMATION

Corresponding Author

*E-mail: miyoshi@kais.kyoto-u.ac.jp. Telephone: +81-75-753-6119. Fax: +81-75-753-6408.

Funding

This work was supported by a Grant-in-Aid for Scientific Research (Grant 23380064 and 26292060 to H.M.) and a Grant-in-Aid for Young Scientists (Grant 23780116 to M.M.) from the Japan Society for the Promotion of Science.

Notes

The authors declare no competing financial interest.

■ ACKNOWLEDGMENTS

We thank Drs. Fumihiko Sato and Kentaro Ifuku (Division of Integrated Life Science, Graduate School of Biostudies, Kyoto University) for allowing us access to their MALDI-TOF MS instrument (Bruker Autoflex III Smartbeam) as well as for their helpful advice on the experiments.

■ ABBREVIATIONS

CBB, Coomassie brilliant blue R250; complex I, proton-translocating NADH-quinone oxidoreductase; DDM, *n*-dodecyl β-maltoside; MALDI-TOF, matrix-assisted laser desorption ionization time-of-flight; MS, mass spectrometry; PVDF, polyvinylidene fluoride; SDS−PAGE, sodium dodecyl sulfate−polyacrylamide gel electrophoresis; SMP, submitochondrial particles; TMH, transmembrane helix.

DOI: 10.1021/acs.biochem.5b00187
Biochemistry 2015, 54, 2739−2746

REFERENCES

(1) Brandt, U. (2006) Energy converting NADH:quinone oxidoreductase (complex I). *Annu. Rev. Biochem. 75*, 69−92.
(2) Hirst, J. (2013) Mitochondrial complex I. *Annu. Rev. Biochem. 82*, 551−575.
(3) Carroll, J., Fearnley, I. M., Skehel, J. M., Shannon, R. J., Hirst, J., and Walker, J. E. (2006) Bovine complex I is a complex of 45 different subunits. *J. Biol. Chem. 43*, 32724−32727.
(4) Baradaran, R., Berrisford, J. M., Minhas, G. S., and Sazanov, L. A. (2013) Crystal structure of the entire respiratory complex I. *Nature 494*, 443−448.
(5) Zickermenn, V., Wirth, C., Nasiri, H., Siegmund, K., Schwalbe, H., Hunte, C., and Brandt, U. (2015) Mechanistic insight from the crystal structure of mitochondrial complex I. *Science 347*, 44−49.
(6) Efremov, R. G., and Sazanov, L. A. (2011) Structure of the membrane domain of respiratory complex I. *Nature 476*, 414−420.
(7) Mathiesen, C., and Hägerhäll, C. (2002) Transmembrane topology of the NuoL, M, and N subunits of NADH:quinone oxidoreductase and their homologues among membrane-bound hydrogenases and *bona fide* antiporters. *Biochim. Biophys. Acta 1556*, 121−132.
(8) Roberts, P. G., and Hirst, J. (2012) The deactive from of respiratory complex I from mammalian mitochondria is a Na^+/H^+ antiporter. *J. Biol. Chem. 287*, 34743−34751.
(9) Tocilescu, M. A., Zickermann, V., Zwicker, K., and Brandt, U. (2010) Quinone binding and reduction by respiratory complex I. *Biochim. Biophys. Acta 1797*, 1883−1890.
(10) Murai, M., Ishihara, A., Nishioka, T., Yagi, T., and Miyoshi, H. (2007) The ND1 subunit constructs the inhibitor binding domain in bovine heart mitochondrial complex I. *Biochemistry 46*, 6409−6416.
(11) Murai, M., Sekiguchi, K., Nishioka, T., and Miyoshi, H. (2009) Characterization of the inhibitor binding site in mitochondrial NADH-ubiquinone oxidoreductase by photoaffinity labeling using a quinazoline-type inhibitor. *Biochemistry 48*, 688−698.
(12) Sekiguchi, K., Murai, M., and Miyoshi, H. (2009) Exploring the binding site of acetogenin in the ND1 subunit of bovine mitochondrial complex I. *Biochim. Biophys. Acta 1787*, 1106−1111.
(13) Kakutani, N., Murai, M., Sakiyama, N., and Miyoshi, H. (2010) Exploring the binding site of Dlac-acetogenin in bovine heart mitochondrial NADH-ubiquinone oxidoreductase. *Biochemistry 49*, 4794−4803.
(14) Murai, M., Mashimo, Y., Hirst, J., and Miyoshi, H. (2011) Exploring interactions between the 49 kDa and ND1 subunits in mitochondrial NADH-ubiquinone oxidoreductase (complex I) by photoaffinity labeling. *Biochemistry 50*, 6901−6908.
(15) Shiraishi, Y., Murai, M., Sakiyama, N., Ifuku, K., and Miyoshi, H. (2012) Fenpyroximate binds to the interface between PSST and 49 kDa subunits in mitochondrial NADH-ubiquinone oxidoreductase. *Biochemistry 51*, 1953−1963.
(16) Tocilescu, M. A., Fendel, U., Zwicker, K., Kerscher, S., and Brandt, U. (2007) Exploring the ubiquinone binding cavity of respiratory complex I. *J. Biol. Chem. 282*, 29514−29520.
(17) Fendel, U., Tocilescu, M. A., Kerscher, S., and Brandt, U. (2008) Exploring the inhibitor binding pocket of respiratory complex I. *Biochim. Biophys. Acta 1777*, 660−665.
(18) Kleyman, T. R., and Cragoe, E. J., Jr. (1988) Amiloride and its analogs as tools in the study of ion transport. *J. Membr. Biol. 105*, 1−21.
(19) Putney, L. K., Denker, S. P., and Barber, D. L. (2002) The changing face of the Na^+/H^+ exchanger, NHE: Structure, regulation, and cellular actions. *Annu. Rev. Pharmacol. Toxicol. 42*, 527−552.
(20) Nakamaru-Ogiso, E., Seo, B. B., Yagi, T., and Matsuno-Yagi, A. (2003) Amiloride inhibition of the proton-translocating NADH-quinone oxidoreductase of mammals and bacteria. *FEBS Lett. 549*, 43−46.
(21) Stolpe, S., and Friedrich, T. (2004) The *Escherichia coli* NADH-ubiquinone oxidoreductase (complex I) is a primary proton pump but may be capable of secondary sodium antiport. *J. Biol. Chem. 279*, 18377−18383.
(22) Murai, M., Habu, S., Murakami, S., Ito, T., and Miyoshi, H. (2015) Production of new amilories as potent inhibitors of mitochondrial respiratory complex I. *Biosci. Biotechnol. Biochem.*, DOI: 10.1080/09168451.2015.1010479.
(23) Ino, T., Nishioka, T., and Miyoshi, H. (2003) Characterization of inhibitor binding sites of mitochondrial complex I using fluorescent inhibitor. *Biochim. Biophys. Acta 1605*, 15−20.
(24) Masuya, T., Murai, M., Ifuku, K., Morisaka, H., and Miyoshi, H. (2014) Site-specific chemical labeling of mitochondrial respiratory complex I through ligand-directed tosylate chemistry. *Biochemistry 53*, 2307−2317.
(25) Matsuno-Yagi, A., and Hatefi, Y. (1985) Studies on the mechanism of oxidative phosphorylation. *J. Biol. Chem. 260*, 14424−14427.
(26) Murai, M., Ichimaru, N., Abe, M., Nishioka, T., and Miyoshi, H. (2006) Mode of inhibitory action of Δlac-acetogenins, a new class of inhibitors of bovine heart mitochondrial complex I. *Biochemistry 45*, 9778−9787.
(27) Laemmli, U. K. (1970) Cleavage of structural proteins during the assembly of the head of bacteriophage T4. *Nature 227*, 680−685.
(28) Schägger, H. (2006) Tricine-SDS-PAGE. *Nat. Protoc. 1*, 16−21.
(29) Rais, I., Kara, M., and Schägger, H. (2004) Two-dimensional electrophoresis for the isolation of integral membrane proteins and mass spectrometric identification. *Proteomics 4*, 2567−2571.
(30) Cleveland, D. W., Fishcher, M. W., Kirschner, M. W., and Laemmli, U. K. (1977) Peptide mapping by limited proteolysis in sodium dodecyl sulfate and analysis by gel electrophoresis. *J. Biol. Chem. 252*, 1102−1106.
(31) Kmita, K., and Zickermann, V. (2013) Accessory subunits of mitochondrial complex I. *Biochem. Soc. Trans. 41*, 1272−1279.
(32) Vinothkumar, K. R., Zhu, P., and Hirst, J. (2014) Architecture of mammalian respiratory complex I. *Nature 515*, 80−84.
(33) Earley, F. G. P., Patel, S. D., Ragan, C. I., and Attardi, G. (1987) Photolabeling of a mitochondrially encoded subunit of NADH dehydrogenase with [^{3}H]dihydrorotenone. *FEBS Lett. 219*, 108−113.
(34) Schuler, F., Yano, T., Bernardo, S. D., Yagi, T., Yankovskaya, V., Singer, T. P., and Casida, J. E. (1999) NADH-quinone oxidoreductase: PSST subunit couples electron transfer from iron-sulfur cluster N2 to quinone. *Proc. Natl. Acad. Sci. U.S.A. 96*, 4149−4153.
(35) Masuya, T., Murai, M., Morisaka, H., and Miyoshi, H. (2014) Pinpoint chemical modification of Asp160 in the 49 kDa subunit of bovine mitochondrial complex I via a combination of ligand-directed tosyl chemistry and click chemistry. *Biochemistry 53*, 7816−7823.
(36) Steuber, J. (2003) The C-terminally trunctuated NuoL subunit (ND5 homologue) of the Na^+-dependent complex I from *Escherichia coli* transports Na^+. *J. Biol. Chem. 278*, 26817−26822.
(37) Davies, K., and Solioz, M. (1992) Assessment of uncoupling by amiloride analogues. *Biochemistry 31*, 8055−8058.

DOI: 10.1021/acs.biochem.5b00187
Biochemistry 2015, 54, 2739−2746